

# The Role of Nitric Oxide in the Pathogenesis of Spontaneous Murine Autoimmune Disease: Increased Nitric Oxide Production and Nitric Oxide Synthase Expression in MRL-*lpr/lpr* Mice, and Reduction of Spontaneous Glomerulonephritis and Arthritis by Orally Administered N<sup>G</sup>-Monomethyl-L-Arginine

By J. Brice Weinberg,\* Donald L. Granger,\*<sup>†</sup> David S. Pisetsky,\*<sup>§</sup> Michael F. Seldin,\*<sup>†</sup> Mary A. Misukonis,\* S. Nick Mason,\* Anne M. Pippen,\* Philip Ruiz,<sup>||</sup> Edgar R. Wood,<sup>¶</sup> and Gary S. Gilkeson\*

From the Departments of \*Medicine, <sup>†</sup>Microbiology, and <sup>§</sup>Immunology, Veterans Administration and Duke University Medical Centers, Durham, North Carolina 27705; the <sup>||</sup>Department of Pathology, University of Miami Medical Center, Miami, Florida 33101; and the <sup>¶</sup>Department of Cell Biology, Burroughs Wellcome Company, Research Triangle Park, North Carolina 27709

## Summary

MRL-*lpr/lpr* mice spontaneously develop various manifestations of autoimmunity including an inflammatory arthropathy and immune complex glomerulonephritis. This study examines the role of nitric oxide, a molecule with proinflammatory actions, in the pathogenesis of MRL-*lpr/lpr* autoimmune disease. MRL-*lpr/lpr* mice excreted more urinary nitrite/nitrate (an in vivo marker of nitric oxide production) than did mice of normal strains and MRL-*+/+* and B6-*lpr/lpr* congenic strains. In addition, MRL-*lpr/lpr* peritoneal macrophages had an enhanced capacity to produce nitric oxide in vitro as well as increased nitric oxide synthase activity, and certain tissues from MRL-*lpr/lpr* mice had increased expression of inducible nitric oxide synthase (NOS) mRNA and increased amounts of material immunoreactive for inducible NOS. Oral administration of N<sup>G</sup>-monomethyl-L-arginine, a nitric oxide synthase inhibitor, prevented the development of glomerulonephritis and reduced the intensity of inflammatory arthritis in MRL-*lpr/lpr* mice. By using interspecific backcross mice, the gene for inducible NOS (*Nosi*) was mapped to mouse chromosome 11. This chromosomal localization was different from those loci that we have previously demonstrated to be linked to enhanced susceptibility to renal disease in an MRL-*lpr/lpr* cross. However, the chromosomal location of the NOS gene was consistent with an insulin-dependent diabetes locus identified in an analysis of nonobese diabetic (NOD) mice. These results suggest that elevated nitric oxide production could be important in the pathogenesis of autoimmunity, and that treatments to block the production of nitric oxide or block its effects might be valuable therapeutically.

MRL-*lpr/lpr* mice develop a spontaneous autoimmune disease characterized by lymphadenopathy, autoantibody production, and inflammatory manifestations including nephritis, vasculitis, and arthritis (1, 2). Immune function abnormalities also include enhanced constitutive macrophage class II antigen expression (3), elevated levels of IFN- $\gamma$ , TNF, IL-1, and IL-6 in isolated kidney, lymph node, and spleen cells (4–6), and an enhanced state of macrophage “activation” (3, 7). These disease manifestations are a result of both a single gene mutation (*lpr*) of the *Fas* apoptosis gene on mouse chro-

mosome 19 (8, 9) and background genes from the MRL strain (1, 9). Although the MRL genes contributing to disease manifestations have not been identified, two loci contributing to renal disease have been mapped to regions of mouse chromosomes 7 and 12 (9).

We have hypothesized that nitric oxide (NO)<sup>1</sup> plays a role

<sup>1</sup> Abbreviations used in this paper: NMMA, N<sup>G</sup>-monoethyl-L-arginine; NO, nitric oxide; NOS, nitric oxide synthase; RFLV, restriction fragment length variants.

in the pathogenesis of disease in MRL-*lpr/lpr* mice. NO, a multifunctional molecule produced by diverse cell types, results from the conversion of L-arginine to L-citrulline and NO by the action of the enzyme nitric oxide synthase (NOS). NO has been noted to promote relaxation of smooth muscle, serve as a neurotransmitter, cause stasis and/or lysis of microbes and tumor cells, and modulate function and differentiation of hematopoietic cells (10–14). NO also has potent proinflammatory actions. Cell-derived NO, through interaction with superoxide, forms peroxynitrite which in turn may spontaneously produce hydroxyl radical, a molecule with high potential for cell and tissue injury and destruction (15–17). NO may increase vascular permeability in inflamed tissues (18). NO has also been shown to cause increased expression of TNF and IL-1 by cells, and to increase the potential of cells to produce hydrogen peroxide (13, 14). Also, rabbit and human chondrocytes have been shown to produce NO and to express iNOS in response to various cytokines and bacterial products (19, 20), and investigators have noted increased concentrations of the NO catabolite nitrite in synovial fluid and sera of patients with inflammatory arthritis (21). McCartney-Francis et al. (22) have recently demonstrated that rats with arthritis induced by injection of streptococcal cell wall fragments have increased production of NO, and that administration of an inhibitor of NO synthase suppresses the arthritis.

In the current studies, we have investigated the role of NO in *lpr* spontaneous autoimmune disease and determined the chromosomal location of iNOS. Results demonstrate that MRL-*lpr/lpr* mice have elevated levels of urinary excretion of nitrite/nitrate (a marker of NO production), and that their macrophages have an enhanced capacity for NO production. Certain tissues from MRL-*lpr/lpr* mice have increased NOS activity, increased expression of iNOS mRNA, and increased amounts of material immunoreactive for iNOS. Furthermore, blocking NO production with *N*<sup>G</sup>-monomethyl-L-arginine (NMMA) prevents the development of inflammatory nephritis and arthritis in these mice. As determined by interspecific backcross experiments, the gene for iNOS maps to mouse chromosome 11. This position is different from the location of *Fas* and those loci that we have previously demonstrated to be significantly linked to susceptibility to renal disease in MRL-*lpr/lpr* mice.

## Materials and Methods

**Mice.** C3H/HeJ (C3H), C3H/H3J-*gld* (C3H-*gld*), BALB/cJ (BALB), C57BL/6J (B6), C57BL/6J-*lpr* (B6-*lpr/lpr*), MRL/MpJ-*lpr* (MRL-*lpr/lpr*), and MRL/MpJ (MRL-+/+) mice were originally obtained from The Jackson Laboratory (Bar Harbor, ME). Based on serological testing, these mice had no evidence of infection with the following murine viruses and mycoplasmas: pneumonia virus of mice, mouse hepatitis virus, Sendai virus, ectromelia virus, mouse rotavirus, lymphocytic choriomeningitis virus, reovirus 3, Theiler's encephalomyelitis virus, minute virus of mice, *Mycoplasma pulmonis*, and *Mycoplasma arthritidis*. Breeding to produce selected F<sub>1</sub> mice (see below) was done in our animal facility.

**Nitrite/Nitrate Assay.** Mice were housed in metabolic cages (three per cage) and fed deionized distilled sterile water and a defined

arginine and nitrate-free diet as noted before (23). Urine was collected into isopropanol to inhibit bacterial growth. Urinary nitrite/nitrate concentration was determined spectrophotometrically as described before (23). Determinations were done in duplicate or triplicate. Total nitrate excretion was then calculated based on the concentration and the urine volume.

**NOS Assay.** Spleen, liver, kidneys, lymph nodes, and peritoneal cells were collected and quickly frozen in a dry ice-ethanol slurry in a buffer-protease inhibitor cocktail containing 100 μM phenylmethylsulfonyl fluoride, 5 μg/ml aprotinin, 1 μg/ml chymostatin, and 5 μg/ml pepstatin A. The tissue cells were then disrupted with a pestle and repeated freeze-thaw cycles. Cytosol was collected after centrifugation, and assayed for protein and NOS activity using a modification of procedures noted before (24, 25). The assay buffer contained 50 mM Hepes (pH 7.5), 200 μM NADPH, 1 mM dithiothreitol, 10 μM FAD, 100 μM tetrahydrobiopterin, and 10 μM L-arginine. We used L-arginine labeled with tritium in the guanidino position (NEC-453; New England Nuclear, Boston, MA). 30 μl of sample was used in a total reaction mixture of 50 μl. Samples were done in duplicate or triplicate.

**Messenger RNA Analysis, Immunofluorescence, and Immunoblots.** Total mRNA extraction and analysis was performed as noted before (6, 14). Indirect immunofluorescence was done as described before on tissues that were frozen quickly, sectioned, and fixed in cold acetone (26). Guinea pig serum containing antibody specific for natural rat iNOS was from Dr. Stephen Gross (Oxford University, Oxford, England). Normal guinea pig serum served as negative control in experiments using the guinea pig antiserum. A rabbit polyclonal antiserum against murine RAW264.7 iNOS was produced by immunization with an iNOS fusion protein expressed in *Escherichia coli*. cDNA encoding amino acids 1–224 of RAW264.7 iNOS was amplified by RNA-PCR as described (25, 27), and inserted into the pGEX2T vector (Pharmacia LKB, Piscataway, NJ). Gene expression from this plasmid construct results in the production of a protein containing 26 kD of the carboxyl terminus of glutathione-S-transferase fused to amino terminus of the encoded region of RAW264.7 iNOS. The iNOS fusion protein was purified from *E. coli* by affinity chromatography on glutathione-Sepharose (Pharmacia LKB) (28) followed by preparative SDS polyacrylamide electrophoresis. The purified iNOS fusion protein in the acrylamide gel band was directly injected into New Zealand rabbits as described (29). Immunoprecipitates and immunoblots using the antiserum were done as described before (29). For the immunoblots, tissue from mouse organs was frozen rapidly in liquid nitrogen. In immunoprecipitation experiments, the tissue was homogenized and extracts were precipitated with the rabbit anti-mouse iNOS antibody.

**Chromosome Localization.** C3H/HeJ-*gld* and *Mus spretus* (Spain) mice and [(C3H/HeJ-*gld* × *Mus spretus*)F<sub>1</sub> × C3H/HeJ-*gld*] interspecific backcross mice were bred and maintained as previously described (30). *Mus spretus* was chosen as the second parent in this cross because of the relative ease of detection of informative restriction fragment length variants (RFLV) in comparison with crosses using conventional inbred laboratory strains.

DNA was isolated from mouse organs by standard techniques. DNA was digested with restriction endonucleases, and 10-μg samples were electrophoresed in 0.9% agarose gels. DNA was transferred Nytran membranes (Schleicher and Schuell, Inc., Keene, NH), hybridized at 65°C, and washed under stringent conditions, as previously described (31). Clones used as probes in the current study included the mouse macrophage iNOS cDNA (nucleotides 1–675 [27, 32]), the avian erythroblastosis a and b (*ErbA* and *ErbB2*) cDNAs, pAEPst0.45 and pAEBam0.5, respectively (33), and the p53 proto-oncogene cDNA (*Trp53*) (34).

Gene linkage was determined by segregation analysis (35). Gene order was determined by analyzing all haplotypes and minimizing crossover frequency between all genes that were determined to be within a linkage group. This method resulted in determination of the most likely gene order (36).

**NMMA Treatment.** Groups of 8-wk-old MRL-*lpr/lpr* mice were given either sterile distilled deionized water or the water containing 50 mM NMMA for ad libitum consumption. NMMA was from CalBiochem-Behring Corp. (San Diego, CA) and from Dr. Owen Griffith (Medical College of Wisconsin, Milwaukee, WI). Both groups of mice were maintained on the defined nitrate-free diet described above. At weekly intervals, the mice were placed in metabolic cages and 24-h urine collections were obtained. Urinary nitrate/nitrite was measured as described above, and urinary protein was measured using the Bradford assay (Bio-Rad Laboratories, Richmond, CA). After 10 wk of treatment, the mice were bled and killed with removal of the kidneys and knee joints.

Serum anti-DNA activity was determined by ELISA as previously described (37). The kidneys were imbedded in paraffin, sectioned, and stained with hematoxylin and eosin. Knee joints were decalcified in formic acid, embedded into paraffin, sectioned, and stained. Slides were then read by a pathologist "blinded" as to the group of origin. The amount of kidney and knee joint disease present in each specimen were quantitated as noted before (38). Briefly, glomeruli were graded for hypercellularity (0-4), hyperlobularity (0-4), crescents (0-4), and necrosis (0-4). A score was then derived by adding the grading of these features of glomerular disease. Kidneys from normal BALB mice usually have scores from 0 to 1. Vasculitis was noted when present in medium size vessels in the kidney sections. The synovial score was derived by adding the grading of synovial proliferation (0-3) and subsynovial inflammation (0-3). Knee joints from normal BALB mice usually have scores from 0 to 0.5.

## Results

**Nitrite/Nitrate Excretion.** In animals consuming a nitrate-free diet, urinary excretion of nitrite/nitrate accurately reflects the endogenous production of NO (23). To determine the production of NO in mice of different strains, we analyzed urine collected daily under basal conditions. Fig. 1 A demonstrates that MRL-*lpr/lpr* mice excrete more nitrite/nitrate than do C3H mice, when analyzed over a 10-d period at 3 mo of age. Likewise, when analyzed over time beginning at 6 wk of age, MRL-*lpr/lpr* mice excrete higher levels of nitrite/nitrate than do B6 mice as the mice age (Fig. 1 B). Higher nitrate/nitrite excretion begins at ~10-12 wk of age, paralleling that of proteinuria (Fig. 1 C). Oral administration of 50 mM NMMA in water to the MRL-*lpr/lpr* mice reduced the high level nitrite/nitrate excretion (see below). This signifies that the nitrite/nitrate is a product of NOS, since NMMA is a specific inhibitor of the enzyme (10, 12, 39). Levels of nitrite/nitrate excretion in 5-mo-old mice of strains MRL-+/+ (0.8  $\mu\text{mol}/\text{mouse per d}$ ) and B6-*lpr/lpr* (1.2  $\mu\text{mol}/\text{mouse per d}$ ) (three mice in each group) were normal. These results indicate that neither the *lpr* gene per se nor the MRL genetic background is adequate for the expression of enhanced nitrite excretion, and that both the *lpr* gene and genetic factors in the MRL background are necessary.

**NO Production In Vitro and Nitric Oxide Synthase Content.** Peritoneal macrophages from the normal BALB mice

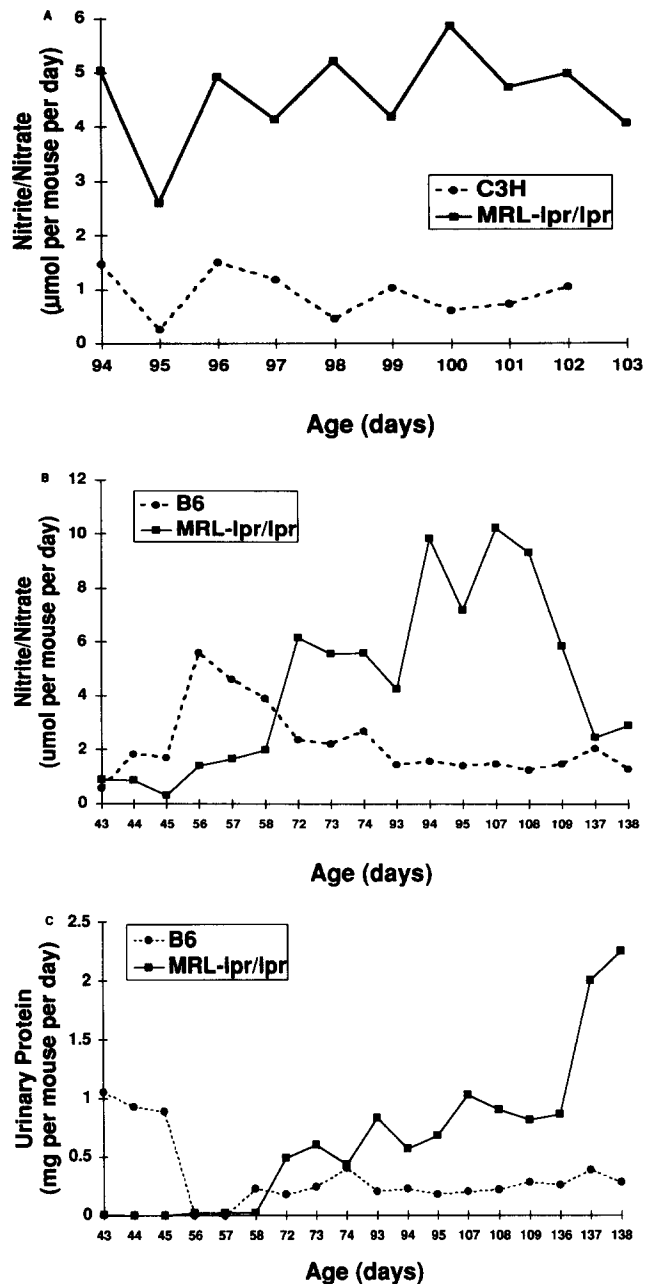


**Figure 1.** Enhanced urinary nitrite/nitrate excretion in MRL-*lpr/lpr* mice. (A) Urinary nitrite/nitrate excretion in 5-mo-old C3H and MRL-*lpr/lpr* mice (three mice in each group). (B) Urinary nitrite/nitrate excretion in B6 and MRL-*lpr/lpr* mice over a longer period of time. The experiment began when the mice were 6 wk old (three mice in each group). (C) Urinary protein in B6 and MRL-*lpr/lpr* (three mice in each group). These figures show results of one set of three experiments that showed comparable results. However, in the results represented in B and C, the initial mildly elevated levels of excretion in B6 mice seen early were noted in only one of three experiments.

had no enhancement of nitrite/nitrate production when treated with endotoxin or IFN- $\gamma$  alone, but the combination enhanced the production greatly. In contrast, peritoneal macrophages from MRL-*lpr/lpr* mice had enhanced responses to treatment with endotoxin and murine IFN- $\gamma$  alone, as well

as with combined endotoxin/IFN- $\gamma$  treatment (Fig. 2). To determine if there was enhanced tissue iNOS mRNA expression, RNA was extracted from organs from BALB and MRL-*lpr/lpr* mice, and then examined by Northern analysis for iNOS mRNA expression (Fig. 3). The iNOS mRNA (~4.7 kb in size) was noted in tissue from kidney and spleen from MRL-*lpr/lpr* mice, but not in those from BALB mice. Various tissues and cells from MRL-*lpr/lpr* and BALB mice were extracted and analyzed for their abilities to convert [ $^{14}$ C]L-arginine (labeled in the guanidino position) to [ $^{14}$ C]L-citrulline. Peritoneal macrophages and spleen extracts from MRL-*lpr/lpr* mice displayed more NOS activity than did those from BALB mice, while the activity in kidney extracts was not different (Fig. 4). By immunofluorescence analysis using a rabbit anti-mouse iNOS antibody, we noted no NOS antigen expression in spleen, liver, and kidney from BALB mice, and none in liver or kidney from MRL-*lpr/lpr* mice. However, spleens from MRL-*lpr/lpr* mice displayed large numbers of cells containing the NOS antigen (Fig. 5 A). Comparable findings were noted when we used a monospecific guinea pig anti-rat inducible NOS antibody (data not shown). When tissue extracts were analyzed for iNOS antigen by immunoprecipitation and immunoblotting techniques using a rabbit anti-mouse iNOS antibody, we did not detect antigen in extracts from organs of BALB mice, although extracts from spleen and kidney tissues from MRL-*lpr/lpr* mice had readily detectable antigen (Fig. 5 B).

**NMMA Treatment.** Groups of MRL-*lpr/lpr* mice received either double distilled water ( $n = 10$ ) or water containing 50 mM NMMA ( $n = 9$ ) beginning at 8 wk of age. Both groups of mice received the defined nitrate free diet. Mice were treated for a total of 10 wk. Mice in both groups appeared clinically normal. However, two mice in the NMMA group died during week 3 of treatment, leaving seven mice in the NMMA group for analysis. Extensive autopsies (including careful histological examinations and culturing of serum, urine, and organs) on these two mice and on a com-

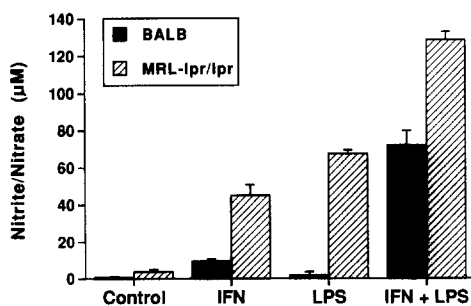


**Figure 2.** Enhanced capacity of peritoneal macrophages from MRL-*lpr/lpr* mice to produce nitrite/nitrate in vitro. Resident peritoneal macrophages were harvested from BALB or MRL-*lpr/lpr* mice and cultured as noted before (59) with the indicated additives (50 ng/ml endotoxin; 50 U/ml IFN- $\gamma$ ). After 48 h of culture, culture supernatant nitrite/nitrate was determined. Means and standard errors of means of triplicate samples are displayed. This figure shows results of one of three experiments; all showed comparable patterns of results.

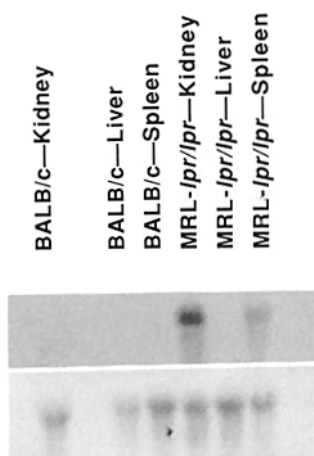


**Figure 3.** Increased expression of mRNA for inducible nitric oxide synthase in samples from MRL-*lpr/lpr* mice. Northern blot analysis was done on total mRNA (20  $\mu$ g/lane) extracted from the indicated tissues and probed with a cDNA for mouse macrophage iNOS cDNA (nucleotides 1-675). The top portion shows the results from the x-ray film after probing with the cDNA. The bottom portion displays the same filter after removing the iNOS cDNA probe, and reanalyzing with a probe for 28S RNA as an indication of the equality of mRNA loading.

parable mouse that had received NMMA for 4 wk revealed no evidence of microbial infection or other evident cause of death. As shown in Fig. 6 A, administration of NMMA in the drinking water of MRL-*lpr/lpr* mice effectively blocked nitrate/nitrite excretion (and by inference nitric oxide production). Also, mice receiving NMMA excreted significantly less protein than did control mice; this difference became apparent at week 5 of treatment (Fig. 6 B).

Pathologic examination of the kidneys and knee joints of mice from the two groups of mice revealed significantly less disease in the NMMA-treated group. Renal disease as measured by the renal score, and arthritis as measured by the synovial score were both significantly less in the NMMA group as compared with the control group (Fig. 7). There was minimal to no glomerular proliferation in mice treated with NMMA, while all but one of the control mice had significant glomerular proliferation and hyperlobulation. The chronic interstitial lymphocytic infiltrate seen in the kidneys of all *lpr* congenic mice (including C3H-*lpr/lpr* mice that do not develop glomerulonephritis) was present to comparable degrees in both control and NMMA-treated mice. Medium vessel vasculitis appears sporadically in the kidneys of untreated MRL-*lpr/lpr* mice with an overall incidence of 30% (40). Mild to moderate (1-2+) medium vessel vasculitis was present in 3 of 10 kidneys from mice in the control group. Mild vasculitis was seen in 1 of 7 kidneys from the NMMA-treated group.

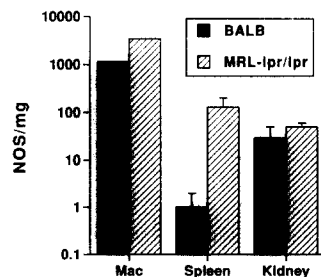


**Figure 4.** Increased expression of NO synthase activity in samples from MRL-*lpr/lpr* mice. NOS functional activity in extracts of peritoneal macrophages (Mac), spleen, and kidney from BALB and MRL-*lpr/lpr* mice. Results are presented on a log scale as pico-moles L-citrulline generated from L-arginine per milligram protein. Means and standard errors of means of duplicate or triplicate samples are displayed.

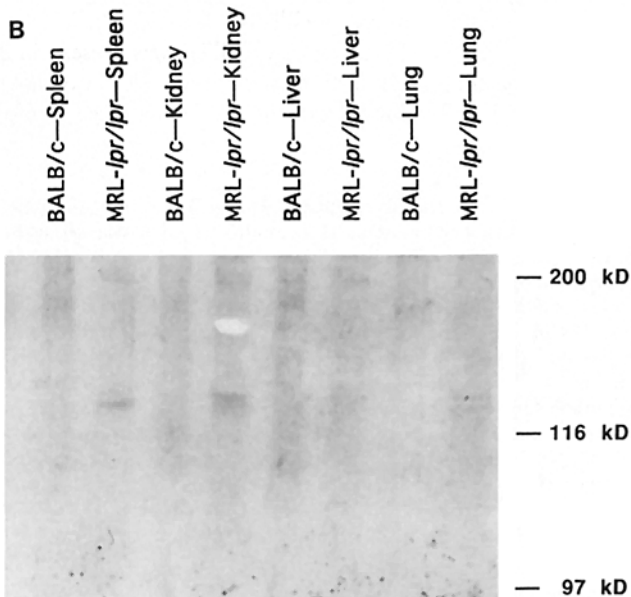
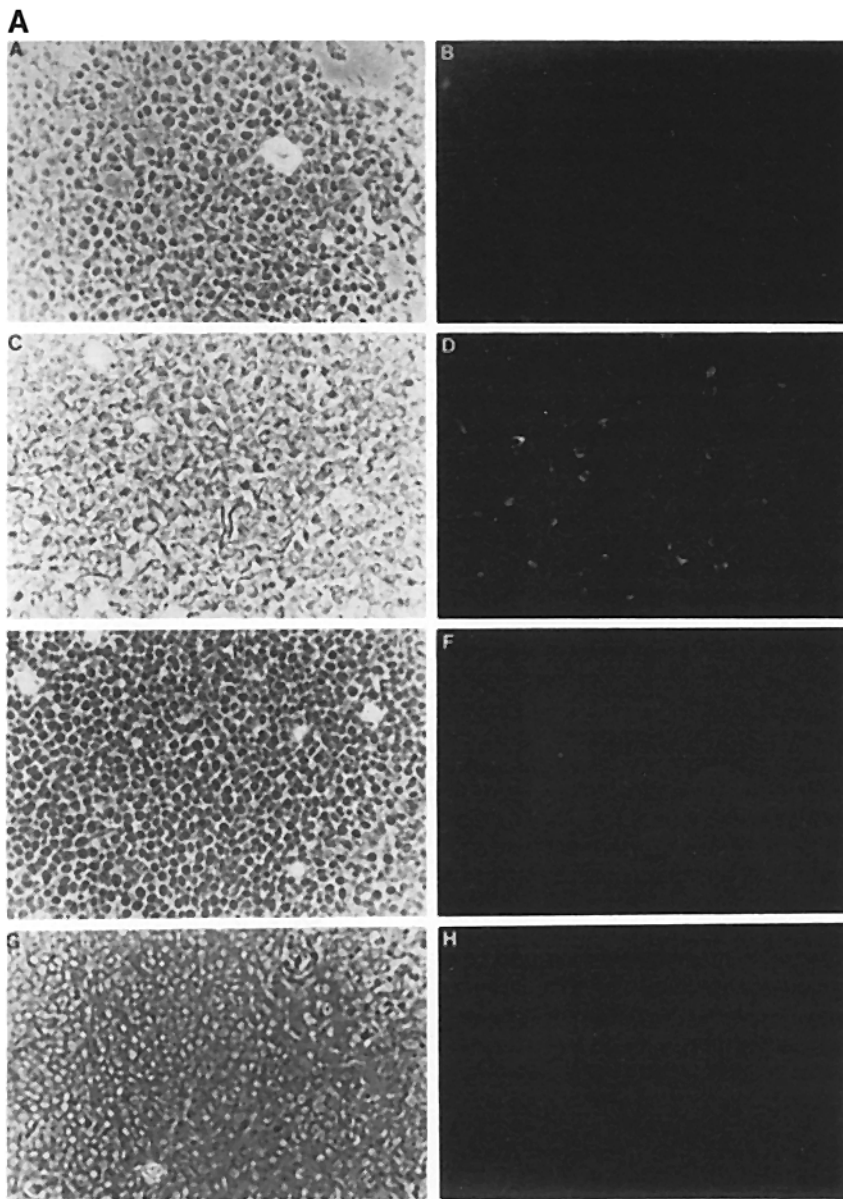


**Figure 5.** Demonstration of iNOS antigen in tissues of MRL-*lpr/lpr* mice. (A) Immunofluorescence of spleen (A and B) and lymph nodes (E and F) from BALB mice and from MRL-*lpr/lpr* mice (C and D [spleen], and G and H [lymph nodes]). A, C, E, and G are phase contrast views of tissue, and B, D, F, and H are fluorescent views of tissue. D demonstrates several spleen cells staining positively for iNOS antigen. Tissues reacted with normal rabbit serum instead of rabbit anti-iNOS serum were negative. These photographs are from one of two different experiments performed; each showed comparable results. (B) Immunoblot of immunoprecipitated material from tissue extracts from BALB and MRL-*lpr/lpr* mice. The lanes containing material of MRL-*lpr/lpr* mice spleen and kidney show positive reactions with bands at approximately 135 kD, while all other lanes are negative. The bars at the right represent the positions of molecular mass markers.

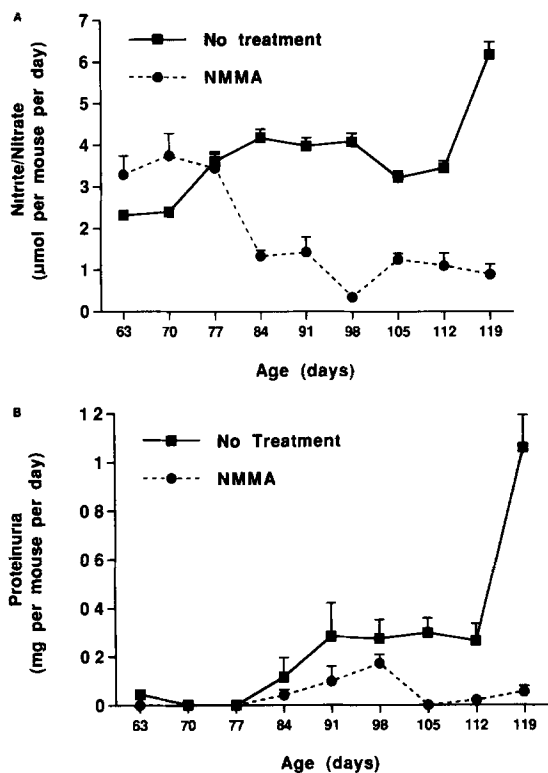
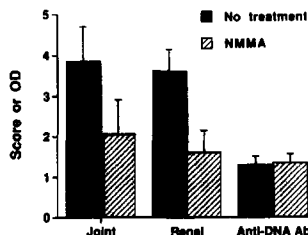


**Figure 6.** Effect of NMMA ingestion on nitrite/nitrate excretion and proteinuria in MRL-*lpr/lpr* mice. (A) Urinary nitrite/nitrate excretion in MRL-*lpr/lpr* mice receiving either water or 50 mM NMMA in water orally ad libitum. Urine determinations were done on urines collected over a 24-h period from mice (two per cage) at the times designated. (B) Proteinuria in MRL-*lpr/lpr* mice receiving either water or 50 mM NMMA in water orally ad libitum. Urine determinations were done on urines collected over a 24-h period from mice (two per cage) at the times designated. Urine nitrite/nitrate determinations were done on the samples collected at the designated time points (samples from five cages in the NO treatment group and four cages in the NMMA group). Means and standard errors of the means are displayed. The observed differences are statistically different ( $p < 0.05$ ) (Mann-Whitney U test) at all points after 77 d of age in A and B.

There was not a statistical difference in vasculitis between the two groups, but the small numbers of mice with vasculitis makes it difficult to draw firm conclusions regarding the effects of NMMA on this aspect of inflammation. Synovial

**Figure 7.** Effect of NMMA ingestion of glomerulonephritis, arthritis, and levels of anti-DNA antibodies in MRL-*lpr/lpr* mice. Means and standard errors of means of scores (for joint and renal) or of OD (for anti-double-stranded DNA antibody) are displayed. The observed differences for joint disease and renal disease are statistically different ( $p < 0.05$  and  $p < 0.022$ , respectively, using the Mann-Whitney U test), while that for anti-DNA antibody level is not.



proliferation was significantly decreased in the mice treated with NMMA (Fig. 7). While only 3 of 7 mice in the NMMA-treated group had abnormal knee joints with mild to moderate synovial proliferation and synovial inflammation, all 10 mice in the control water group had some degree of synovial proliferation and inflammation. Levels of serum anti-double-stranded DNA measured at age 18 wk in the two groups were essentially equivalent (Fig. 7).

**Mouse Chromosomal Localization and Fine Mapping.** To determine the chromosomal location of the gene encoding iNOS (designated *Nosi*) and its relationship to disease susceptibility genes, we analyzed a panel of DNA samples from an interspecific cross that has been characterized for over 500 genetic markers throughout the genome. The genetic markers included in this map span between 50 and 80 cM on each mouse autosome and the X chromosome (for examples, see references 41 and 42). Initially, DNA from the two parental mice [(C3H-*gld* × *Mus spretus*)F<sub>1</sub>] were digested with various restriction endonucleases and hybridized with *Nosi* cDNA probe to determine RFLVs to allow haplotype analysis. Informative

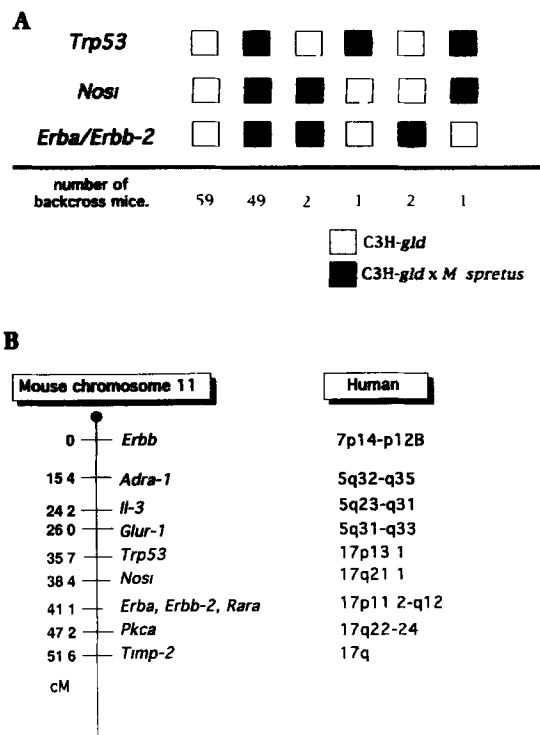


**Figure 8.** Linkage analysis of iNOS. (A) Segregation of *Nosi* among mouse distal mouse chromosome 11 loci in [(C3H-*gld* × *Mus spretus*)F<sub>1</sub> × C3H-*gld*] backcross mice. Closed boxes represent the homozygous C3H pattern and open boxes the F<sub>1</sub> pattern. The RFLVs and haplotype distribution of *ErbB*, and *Erba* in this mouse cross were reported previously (43). For *Trp*, RFLV were detected using BamH1 (C3H-*gld*, 11.0 kb; *Mus spretus*, 18.0 kb). (B) Proposed mouse (and corresponding human) chromosomal localization. *ErbB*, avian erythroblastosis oncogene B, epidermal growth factor receptor; *Adra-1*, adrenergic receptor, alpha-1; *Il-3*, interleukin 3; *Glur-1*, glutamate receptor-1; *Trp53*, transformation-related protein 53; *Nosi*, inducible nitric oxide synthase; *Erba*, avian erythroblastosis oncogene A, thyroid hormone receptor; *Erbb-2*, avian erythroblastosis oncogene B-2, *Rara*, retinoic acid receptor, alpha, *Pkca*, protein kinase C, alpha; *Timp-2*, tissue inhibitor of metalloproteinases-2.

RFLVs were detected with PstI-restricted DNAs: C3H-*gld*, 6.5 kb; *Mus spretus*, 4.8 kb.

Comparison of the haplotype distribution of *Nosi* indicated that in 111 of the 114 meiotic events examined, the *Nosi* locus cosegregated with the erythroblastosis hydroxylase locus (*Erba*), a locus previously mapped to distal mouse chromosome 11 in this cross (Fig. 8 A) (43). The best gene order plus or minus the standard deviation (35, 36) indicated the following relationships from proximal to distal: *Trp53*—2.6 ± 1.5 cM—*Nosi*—2.6 ± 1.5 cM—*Erb2/Erba* (Fig. 8 B).

## Discussion

We demonstrate here that MRL-*lpr/lpr* mice spontaneously excrete high levels of urinary nitrite/nitrate that correspond temporally to the expression of inflammatory disease. Because there is no source of ingested nitrite/nitrate, the urinary nitrite/nitrate represents an oxidation product of NO. MRL-*lpr/lpr* mice also have increased expression iNOS mRNA and of the functional enzyme NOS, and by immunofluorescence and immunoblot assays, they display increased amounts of iNOS antigen in spleen and kidney. Furthermore, treatment with oral NMMA either prevented or significantly decreased clinical autoimmune disease (glomerulonephritis and arthritis), without altering serum levels of anti-DNA antibodies. This result indicates that NO is a critical mediator in the development of the inflammation characteristic of *lpr* disease, and that its production is not simply a reflection of nonspecific immune activation. The efficacy of NMMA suggests that treatments to reduce NO production or NO actions will be beneficial in inflammatory diseases.

The cause(s) for the high levels of iNOS expression and NO production is not known. Mice with various infections have increased NO production (11, 12, 23). Although it is possible that the MRL-*lpr/lpr* mice had a subclinical infection, we feel this is unlikely since they were housed in identical conditions to control strains that had normal nitrate excretion, they had no serological evidence of viral or mycoplasmal infection, and they did not appear to be clinically infected.

MRL-*lpr/lpr* mice have been shown before to display various parameters of macrophage activation (4–8), possibly reflecting high levels of cytokines that may “activate” the macrophages within these animals. The main cytokines thought to be involved are IFN- $\gamma$ , TNF, and IL-1 (4–7). These cytokines are responsible for increasing iNOS and inducing NO production in vivo (10–12). The lack of enhanced nitrite excretion in MRL-+/+ and B6-*lpr/lpr* mice indicates that both the *lpr* gene and other genes in the MRL background are necessary for enhanced iNOS expression.

By using interspecific backcross mapping techniques, we localized the gene for *Nosi* to distal mouse chromosome 11. The position of *Nosi* among other mouse chromosome 11 loci (44) strongly suggests that this gene is located close to the position of the gene for myeloperoxidase, an oxidative enzyme which (like iNOS) is involved in inflammation and host defense. However, a GenBank search showed no homologies in the sequences of iNOS and myeloperoxidase. We

speculate that the close linkage of these genes may reflect some aspect of coordinate regulation.

Based on known chromosomal analogies among positions on mouse and human chromosomes, the position of *Nosi* among other mouse chromosome 11 loci strongly suggests that the human homologue of this gene will be mapped to human chromosome 17 (44). The conserved linkage relationships suggest that this gene will map close to *BRCA1*, a locus linked to familial breast and ovarian cancer on the long arm of human chromosome 17 (45, 46), and to the genes for macrophage inflammatory protein 1- $\alpha$  and 1- $\beta$  (44, 47, 48). A prior report has shown that the gene for constitutive NOS is on human chromosome 12 (49). The location of *Nosi* does not correspond to the sites of loci previously linked to renal disease susceptibility in MRL-*lpr/lpr* mice (9). This result suggests that enhanced iNOS expression and NO production, while critical for the development of disease, may not result from an abnormality in the iNOS gene, per se.

Since MRL-*lpr/lpr* mice have been noted to have high levels of circulating immune complexes (DNA-anti-DNA complexes), it is possible that the immune complexes could result in activation of cells for enhanced iNOS activity and NO production. Mulligan et al. (50, 51) have noted that in rat models of IgG- or IgA-immune complex models of skin and lung inflammation, the NOS inhibitor NMMA can abrogate inflammation. In association with the reduction of inflammation by NMMA in IgG-immune complex lung disease, this compound also reduced the accumulation of alveolar fluid nitrite (51). Furthermore, NMMA administration markedly reduced the accumulation of alveolar macrophages in IgA-immune complex-induced lung disease (50). Similarly, MRL-*lpr/lpr* renal disease is immune complex mediated, primarily by deposition of anti-DNA antibodies. Despite the presence of high serum levels of anti-DNA antibodies, mice receiving NMMA did not develop glomerulonephritis. These studies further support the contention that NO may be important in immunologically induced inflammation.

Other investigators have noted that NO produced by macrophages or pancreatic beta cells is capable of destroying the beta cells and contributing to the development of insulin-dependent diabetes mellitus (52–54). Kleemann et al. (55) showed that adult rats of the insulin-dependent diabetes-prone strain BB have pancreases that display iNOS mRNA and protein coincident with macrophage infiltration and insulinitis, whereas normal rats do not. In a mouse model for insulin-dependent diabetes mellitus (the NOD mouse [56]), researchers have found various genes that influence the development of diabetes. NOD mice have features of an autoimmune disease including anti-islet cell antibodies and defects in T cell activity. Several genetic susceptibility loci have been mapped; these include areas in the major histocompatibility complex in mouse chromosome 17, and sites on chromosomes 1, 3, and 11 (52, 53). The *Idd-5* gene maps to a region on chromosome 1 that includes the genes for the IL-1 receptor and the *Bcg* locus (53). The *Bcg* locus determines the natural resistance (mediated by macrophages) of mice to infection with intracellular microorganisms such as mycobacteria and listeria.

Recently, a strong candidate for *Bcg* has been isolated and

determined to encode a protein with structural homology to membrane proteins that serve to transport nitrate (57). Vidal et al. (57) have found defects in this gene in mice of strains that lack resistance to infection, and they have postulated that these defects might interrupt a system that allows effector cells to accumulate nitrate for conversion to NO, and thus be important in microbial killing. *Idd-4*, a gene that influences the age at which NOD mice develop diabetes, maps to a region on chromosome 11 (58) that corresponds to the region where we map the gene for iNOS. Therefore, we suggest that iNOS is a strong candidate for an insulin dependent diabetes susceptibility gene.

In two autoimmune diseases (that of NOD mice and that of MRL-*lpr/lpr* mice), there are provocative relationships to NO and NOS. NO could act as an effector in promoting inflammation in these mice. Possible proinflammatory effects

of NO include an ability to increase vascular permeability in inflamed tissues (18), the secondary generation of destructive free radicals such as peroxynitrite and hydroxyl radical (15–17), and the induction of the inflammatory cytokines TNF and IL-1 (13, 14). Farrell et al. (21) demonstrated that humans with rheumatoid arthritis and osteoarthritis had increased levels of the NO catabolite nitrite in their synovial fluids and in their sera, suggesting a similar state of increased NO production as in mice with immune inflammation and arthritis. The regional or systemic use of agents that can inhibit the action of NO (e.g., heme-containing compounds such as hemoglobin or myoglobin [12], or agents that can block the production of NO (e.g., the iNOS inhibitor NMMA [22, 39, 50, 51] we used here) could be valuable in therapy in humans with diseases such as systemic lupus erythematosus, rheumatoid arthritis, or insulin-dependent diabetes mellitus.

---

This work was supported in part by the Veterans Administration Research Service (J. B. Weinberg and D. S. Pisetsky), the James R. Swiger Hematology Research Fund (J. B. Weinberg), and National Institutes of Health grants AR-39162 (J. B. Weinberg, G. S. Gilkeson, D. S. Pisetsky, and M. F. Seldin), AR-41053 (M. F. Seldin), and AI-26188 (D. L. Granger). G. S. Gilkeson is an Investigator of the Arthritis Foundation.

Address correspondence to Dr. J. Brice Weinberg, Department of Medicine, VA and Duke University Medical Center, Durham, NC 27705.

Received for publication 13 September 1993 and in revised form 28 October 1993.

## References

- Cohen, P.L., and R.A. Eisenberg. 1991. *Lpr* and *gld*: single gene models of systemic autoimmunity and lymphoproliferative disease. *Annu. Rev. Immunol.* 9:243.
- Andrews, B.S., R.A. Eisenberg, A.N. Theofilopoulos, S. Izui, C.B. Wilson, P.J. McConahey, E.D. Murphy, J.B. Roths, and F.J. Dixon. 1978. Spontaneous murine lupus-like syndromes. Clinical and immunopathological manifestations in several strains. *J. Exp. Med.* 148:1198.
- Lu, C.Y., and E.R. Unanue. 1982. Spontaneous T-cell lymphokine production and enhanced macrophage Ia expression and tumoricidal activity in MRL-*lpr* mice. *Clin. Immunol. Immunopathol.* 25:213.
- Murray, L.J., R. Lee, and C. Martens. 1990. *In vivo* cytokine gene expression in T cell subsets of the autoimmune MRL/Mp-*lpr/lpr* mouse. *Eur. J. Immunol.* 20:163.
- Manolios, N., L. Schrieber, M. Nelson, and C.L. Geczy. 1989. Enhanced interferon-gamma (IFN) production by lymph node cells from autoimmune (MRL/l, MRL/n) mice. *Clin. Exp. Immunol.* 76:301.
- Boswell, J.M., M.A. Yui, D.W. Burt, and V.E. Kelley. 1988. Increased tumor necrosis factor and IL-1 $\beta$  gene expression in the kidneys of mice with lupus nephritis. *J. Immunol.* 141:3050.
- Dang-Vu, A.P., D.S. Pisetsky, and J.B. Weinberg. 1987. Functional alterations of macrophages in autoimmune MRL-*lpr/lpr* mice. *J. Immunol.* 138:1757.
- Watanabe-Fukunaga, R., C.I. Brannan, N.G. Copeland, N.A. Jenkins, and S. Nagata. 1992. Lymphoproliferation disorder in mice explained by defects in Fas antigen that mediates apoptosis. *Nature (Lond.)* 356:314.
- Watson, M. L., J.K. Rao, G.S. Gilkeson, P. Ruiz, E.M. Eicher, D.S. Pisetsky, A. Matsuzawa, J.M. Rochelle, and M.F. Seldin. 1992. Genetic analysis of MRL-*lpr* mice: relationship of the *Fas* apoptosis gene to disease manifestations and renal disease-modifying loci. *J. Exp. Med.* 176:1645.
- Nathan, C. 1992. Nitric oxide as a secretory product of mammalian cells. *FASEB (Fed. Am. Soc. Exp. Biol.) J.* 6:3051.
- Nathan, C.F., and J.B. Hibbs, Jr. 1991. Role of nitric oxide synthesis in macrophage antimicrobial activity. *Curr. Opin. Immunol.* 3:65.
- Moncada, S., R.M.J. Palmer, and E.A. Higgs. 1991. Nitric oxide: physiology, pathophysiology and pharmacology. *Pharmacol. Rev.* 43:109.
- Lander, H.M., P. Sehajpal, D.M. Levine, and A. Novogrodsky. 1993. Activation of human peripheral blood mononuclear cells by nitric oxide-generating compounds. *J. Immunol.* 150:1509.
- Magrinat, G., S.N. Mason, P.S. Shami, and J.B. Weinberg. 1992. Nitric oxide modulation of human leukemia cell differentiation and gene expression. *Blood.* 80:1880.
- Beckman, J.S., T.W. Beckman, J. Chen, P.A. Marshall, and B.A. Freeman. 1990. Apparent hydroxyl radical production by peroxynitrite: implications for endothelial injury from nitric oxide and superoxide. *Proc. Natl. Acad. Sci. USA.* 87:1620.
- Ischiropoulos, H., L. Zhu, and J.S. Beckman. 1992. Peroxynitrite formation from macrophage-derived nitric oxide. *Arch. Biochem. Biophys.* 298:446.
- Zhu, L., C. Gunn, and J.S. Beckman. 1992. Bactericidal activity of peroxynitrite. *Arch. Biochem. Biophys.* 298:452.
- Mayhan, W.G. 1992. Role of nitric oxide in modulating per-



- meability of hamster cheek pouch in response to adenosine 5'-diphosphate and bradykinin. *Inflammation*. 16:295.
19. Stadler, J., M. Stefanovic-Racic, T.R. Billiar, R.D. Curran, L.A. McIntyre, H.I. Georgescu, R.L. Simmons, and C.H. Evans. 1991. Articular chondrocytes synthesize nitric oxide in response to cytokines and lipopolysaccharide. *J. Immunol.* 147:3915.
  20. Palmer, R.M.J., M.S. Hickery, I.G. Charles, S. Moncada, and M.T. Bayliss. 1993. Induction of nitric oxide synthase in human chondrocytes. *Biochem. Biophys. Res. Commun.* 193:398.
  21. Farrell, A.J., D.R. Blake, R.M.J. Palmer, and S. Moncada. 1992. Increased concentrations of nitrite in synovial fluid and serum samples suggest increased nitric oxide synthesis in rheumatic diseases. *Ann. Rheum. Dis.* 51:1219.
  22. McCartney-Francis, N., J.B. Allen, D.E. Mizel, J.E. Albina, Q.-w. Xie, C.F. Nathan, and S.M. Wahl. 1993. Suppression of arthritis by an inhibitor of nitric oxide synthase. *J. Exp. Med.* 178:749.
  23. Granger, D.L., J.B. Hibbs, Jr., and L.M. Broadnax. 1991. Urinary nitrate excretion in relation to murine macrophage activation. Influence of dietary L-arginine and oral N<sup>G</sup>-monomethyl-L-arginine. *J. Immunol.* 146:1294.
  24. Bredt, D.S., and S.H. Snyder. 1989. Nitric oxide mediates glutamate-linked enhancement of cGMP levels in the cerebellum. *Proc. Natl. Acad. Sci. USA.* 86:9030.
  25. Sherman, P.A., V.E. Laubach, B.R. Reep, and E.R. Wood. 1993. Purification and cloning of a cytokine-induced nitric oxide synthase from a human tumor cell line. *Biochemistry.* 32:11600.
  26. Weinberg, J.B., A.M.M. Pippen, and C.S. Greenberg. 1991. Extravascular fibrin formation and dissolution in synovial tissue of patients with osteoarthritis and rheumatoid arthritis. 1991. *Arthritis Rheum.* 34:996.
  27. Wood, E.R., H. Berger, Jr., P.A. Sherman, and E.G. Lapetina. 1993. Hepatocytes and macrophages express an identical cytokine inducible nitric oxide synthase gene. *Biochem. Biophys. Res. Commun.* 191:767.
  28. Smith, D.B., and L.M. Corcoran. 1990. Expression and purification of glutathione-S-transferase fusion proteins. In *Current Protocols in Molecular Biology*. F.M. Ausubel, R. Brent, R.E. Kingston, D.D. Moore, J.G. Seidman, J.A. Smith, and K. Struhl, editors. John Wiley and Sons, Inc., New York. 16.7.
  29. Harlow, E., and D. Lane. 1988. *Antibodies. A Laboratory Manual*. Cold Spring Harbor Press, Cold Spring Harbor, NY. 726 pp.
  30. Seldin, M.F., H.C. Morse, III., J.P. Reeves, C.L. Scribner, R.C. LeBoeuf, and A.D. Steinberg. 1988. Genetic analysis of autoimmune *gld* mice. I. Identification of a restriction fragment length polymorphism closely linked to the *gld* mutation within a conserved linkage group. *J. Exp. Med.* 167:688.
  31. Maniatis, T., E. F. Fritsch, and J. Sambrook. 1982. *Molecular Cloning: A Laboratory Manual*. Cold Spring Harbor Laboratory, Cold Spring, NY. 520 pp.
  32. Lyons, C.R., G.J. Orloff, and J.M. Cunningham. 1992. Molecular cloning and functional expression of an inducible nitric oxide synthase from a murine macrophage cell line. *J. Biol. Chem.* 267:6370.
  33. Vennstom, B., and J.M. Bishop. 1982. Isolation and characterization of chicken DNA homologous to the two putative oncogenes of avian erythroblastosis virus. *Cell.* 28:135.
  34. Jenkins, J.R., K. Rudge, S. Redmond, and A. Wade-Evans. 1984. Cloning and expression analysis of full length mouse cDNA sequences encoding the transformation associated protein p53. *Nucleic Acids Res.* 12:5609.
  35. Green, E.L. 1981. Linkage, recombination and mapping. In *Genetics and Probability in Animal Breeding Experiments*. E. Green, editor. Macmillan Publishing Co., New York. 77-113.
  36. Bishop, D.T. 1985. The information content of phase-known matings for ordering genetic loci. *Genet. Epidemiol.* 2:349.
  37. Gilkeson, G.S., J.P. Grudier, D.G. Karounos, and D.S. Pisetsky. 1989. Induction of anti-double stranded DNA antibodies in normal mice by immunization with bacterial DNA. *J. Immunol.* 142:1482.
  38. Gilkeson, G.S., P. Ruiz, J.P. Grudier, R.J. Kurlander, and D.S. Pisetsky. 1989. Genetic control of inflammatory arthritis in congenic lpr mice. *Clin. Immunol. Immunopathol.* 53:460.
  39. Hibbs, J.B., Jr., Z. Vavrin, and R.R. Taintor. 1987. L-arginine is required for expression of the activated macrophage effector mechanism causing selective metabolic inhibition in target cells. *J. Immunol.* 138:550.
  40. Gilkeson, G.S., R. Spurney, T.M. Coffman, R. Kurlander, P. Ruiz, and D.S. Pisetsky. 1992. Effect of anti-CD4 antibody treatment on inflammatory arthritis in MRL-lpr/lpr mice. *Clin. Immunol. Immunopathol.* 64:166.
  41. Watson, M.L., P. D'Eustachio, B.A. Mock, A.D. Steinberg, H.C. Morse, R.J. Oakey, T.A. Howard, J.M. Rochelle, and M.F. Seldin. 1992. A linkage map of mouse chromosome 1 using an interspecific cross segregating for the *gld* autoimmunity mutation. *Mamm. Genome.* 2:158.
  42. Saunders, A.M., and M.F. Seldin. 1990. A molecular genetic linkage map of mouse chromosome 7. *Genomics.* 8:525.
  43. Oakey, R.J., M.G. Caron, R.J. Lefkowitz, and M.F. Seldin. 1991. Genomic organization of adrenergic and serotonin receptors in the mouse: linkage mapping of sequence-related genes provides a method for examining mammalian chromosome evolution. *Genomics.* 10:338.
  44. Buchberg, A.M., M.S. Buckwalter, and S.A. Camper. 1992. Mouse chromosome 11. *Mamm. Genome.* 3:S162.
  45. Hall, J.M., M.K. Lee, B. Newman, J.E. Morrow, L.A. Anderson, B. Huey, and M.-C. King. 1990. Linkage of early-onset familial breast cancer to chromosome 17q21. *Science (Wash. DC).* 250:1684.
  46. Narod, S.A., J. Feunteun, H.T. Lynch, P. Watson, T. Conway, J. Lynch, and G.M. Lenoir. 1991. Familial breast-ovarian cancer locus on chromosome 17q12-q23. *Lancet.* 338:82.
  47. Wilson, S.D., P.R. Billings, P. D'Eustachio, R.E.K. Fournier, E. Geissler, P.A. Lalley, P.R. Burd, D.E. Housman, B.A. Taylor, and M.E. Dorf. 1990. Clustering of cytokine genes on mouse chromosome 11. *J. Exp. Med.* 171:1301.
  48. Irving, S.G., P.F. Zipfel, J. Balke, O.W. McBride, C.C. Morton, P.R. Burd, U. Siebenlist, and K. Kelly. 1990. Two inflammatory mediator cytokine genes are closely linked and variable amplified on chromosome 17q. *Nucleic Acids Res.* 18:3261.
  49. Kishimoto, J., N. Spurr, M. Liao, L. Lizhi, P. Emson, and W. Xu. 1992. Localization of brain nitric oxide synthase (NOS) to human chromosome 12. *Genomics.* 14:802.
  50. Mulligan, M.S., J.S. Warren, C.W. Smith, D.C. Anderson, C.G. Yeh, A.R. Rudolph, and P.A. Ward. 1992. Lung injury after deposition of IgA immune complexes. Requirements for CD18 and L-arginine. *J. Immunol.* 148:3086.
  51. Mulligan, M.S., J.M. Hevel, M.A. Marletta, and P.A. Ward. 1991. Tissue injury caused by deposition of immune complexes is L-arginine dependent. *Proc. Natl. Acad. Sci. USA.* 88:6338.
  52. Garchon, H.-J., P. Bedossa, L. Eloy, and J.-F. Bach. 1991. Identification and mapping to chromosome 1 of a susceptibility locus for periinsulinitis in non-obese diabetic mice. *Nature (Lond.).* 353:260.
  53. Cornall, R.J., J.-B. Prins, J.A. Todd, A. Pressey, N.H.

- DeLarato, L.S. Wicker, and L.B. Peterson. 1991. Type 1 diabetes in mice is linked to the interleukin-1 receptor and *Lsh/Ity/Bcg* genes on chromosome 1. *Nature (Lond.)* 353:262.
54. Kolb, H., and V. Kolb-Bachofen. 1992. Type 1 (insulin-dependent) diabetes mellitus and nitric oxide. *Diabetologia* 35:796.
55. Kleemann, R., H. Rothe, V. Kolb-Bachofen, Q.-W. Xie, C. Nathan, S. Martin, and H. Kolb. 1993. Transcription and translation of inducible nitric oxide synthase in the pancreas of prediabetic BB rats. *FEBS (Fed. Eur. Biochem. Soc.) Lett.* 328:9.
56. Leiter, E.H., M. Prochazka, and D.L. Coleman. 1987. The nonobese diabetic (NOD) mouse. *Am. J. Path.* 128:380.
57. Vidal, S.M., D. Malo, K. Vogan, E. Skamene, and P. Gros. 1993. Natural resistance to infection with intracellular parasites: isolation of a candidate for *Bcg*. *Cell* 73:469.
58. Todd, J.A., T.J. Aitman, R.J. Cornwall, S. Ghosh, J.R.S. Hall, C.M. Hearne, A.M. Knight, J.M. Love, M.A. McAleer, J.-B. Prins, et al. 1991. Genetic analysis of autoimmune type 1 diabetes mellitus in mice. *Nature (Lond.)* 351:542.
59. Weinberg, J.B., and M.A. Misukonis. 1983. Phorbol diester-induced H<sub>2</sub>O<sub>2</sub> production by peritoneal macrophages. Different H<sub>2</sub>O<sub>2</sub> production by macrophages from normal and BCG-infected mice despite comparable phorbol diester receptors. *Cell. Immunol.* 80:405.